

Gliding Robotic Fish: An Underwater Sensing Platform and Its Spiral-Based Tracking in 3D Space

AUTHORS

Feitian Zhang

Department of Electrical and
Computer Engineering, George
Mason University

Osama Ennasr

Xiaobo Tan

Department of Electrical and
Computer Engineering, Michigan
State University

Introduction

Autonomous underwater robots are drawing increasing attention in aquatic scientific research and applications. Application examples include marine sciences, tracking oil spills, monitoring harmful algal blooms, and tracking fish movements, to name just a few. To be successful in such applications, the robots need to be both highly energy-efficient and highly maneuverable to maintain sustained field operation and suit for versatile environments (Tan, 2011).

Gliding robotic fish have emerged recently as a new type of underwater robot for underwater sensing (Zhang et al., 2016a). Such a robot combines the desirable features of both an underwater glider and a robotic fish, which are well known for energy efficiency (Mitchell et al., 2013; Sherman et al., 2001; Webb et al., 2001; Zhang et al., 2014) and maneuvering flexibility (Chen et al., 2010; Morgansen et al., 2007; Phamduy et al., 2015; Zhang et al., 2015), respectively.

ABSTRACT

Gliding robotic fish are a new type of underwater robot that combines the advantages of energy efficiency of underwater gliders and high maneuverability of robotic fish. Tail-enabled spiraling, as a novel locomotion pattern of gliding robotic fish, uses a buoyancy-driven mechanism and features a small turning radius. This paper investigates the spiral trajectory characteristics from the viewpoint of differential geometry and exploits them for curve tracking in the 3D space. The influences of control inputs on spiral trajectories are investigated through both simulation and experiments. A simulation example using a combined feedforward and feedback controller illustrates the proposed curve-tracking approach.

Keywords: gliding robotic fish, spiraling motion, curve tracking, differential geometry

Like underwater gliders, a gliding robotic fish realizes most of its locomotion through buoyancy-driven gliding along with adjustment of its center of gravity to achieve a certain pitch. It uses actively controlled fins to achieve high maneuverability, during turning and orientation maintenance. Of course, fins can also provide additional propulsive power during locomotion, if needed.

Three-dimensional curve tracking is of importance to underwater robots in various applications, such as sampling water columns, locating the pollutant source, and mapping the 3D distributions of biophysical processes underwater. There has been extensive work on dynamics and control in the longitudinal plane for underwater robots without propellers, like underwater gliders, where typically the absence of lateral motion is assumed (Leonard & Graver, 2001; Graver, 2005; Bhatta & Leonard, 2008; Zhang

& Tan, 2015). There has also been some limited research into three-dimensional gliding involving lateral motion, most of which focuses on the steady-state turning or spiraling (Mahmoudian et al., 2010; Zhang et al., 2013). However, little work has been reported on the three-dimensional dynamic motion, particularly, on the curve-tracking problem. The conventional method of position tracking uses Cartesian coordinates directly as reference signals in tracking control. The method is not effective for gliding robotic fish because of the strong nonlinear coupling between the control inputs and the complexity in controller design that arises from the complicated mapping from the control inputs to the robot locomotion. In this paper, we propose to achieve three-dimensional curve tracking by decomposing the desired trajectory into continuously evolving spirals and then tracking those spirals utilizing

the differential geometric features of the spiraling motion.

We first describe the design and development of a gliding robotic fish prototype. Then we will look into the influences of control inputs on the spiraling trajectory characteristic parameters in the sense of differential geometry, which are further validated in experiments. The concept of three-dimensional curve tracking via following evolving spirals will be demonstrated with a simulation example using a combined feedforward and feedback controller.

Implementation of Gliding Robotic Fish

Integrating an actively controlled tail into the miniature underwater glider (Zhang et al., 2014), we have

developed a series of fully functioning gliding robotic fish, named “Grace,” as shown in Figure 1. The robot “Grace 1.0” has been tested in the Kalamazoo River, Michigan, to sample the oil concentration near the site of a 2010 oil spill (Figure 1a). It also has been tested in the Wintergreen Lake, Michigan, to study the harmful algae bloom (HAB) distribution in collaboration with aquatic ecologists (Figure 1b). Most recently, “Grace 2.0” has been field-tested in the Higgins Lake, Michigan, to examine its potential for tracking fish movement using acoustic telemetry (Figure 1c).

This paper will focus on Grace 1.0, which will be just referred to as “Grace”; Grace 2.0 shares basic design concepts but with more advanced functionalities such as a modular sensor payload architecture and better serviceability. The robot Grace has

three actuation systems for locomotion, including the buoyancy system, the mass distribution system, and the actively controlled tail fin system.

In the buoyancy system, water is pumped in and out of the robot’s body to change the net buoyancy. When the robot is heavier than the water it displaces (negatively buoyant), the robot will descend, and when it is lighter than the water it displaces (positively buoyant), the robot will ascend. The pumping system of Grace is enabled by a linear actuator with integrated feedback (ServoCity HDA4-30), which allows precise control of water volume despite the pressure differences at different depths.

For the mass distribution system, another linear actuator (Firgelli L16-140-63-12-P) is used to push a mass (Batteryspace 18.5V Polymer-Li-Ion battery pack) back and forth along a guiding rail to change the center of the mass for the purpose of manipulating the pitch angle.

The fish-like tail fin system in Grace is driven by a servo motor (Hitec Servo HS-7980TH) through a chain transmission. In the three-dimensional locomotion, a deflected tail can also be used to control the turning motion and heading orientation. Like a real fish, the robot can also flap the tail to realize the swimming motion (Figure 1b).

Grace is equipped with navigation sensors and environmental monitoring sensors. Inertial measurement units (IMUs) such as gyro (ST LPY503AL), accelerometer (ST LSM303DLH), and digital compass (ST LSM303DLH) are used to measure the robot’s angular rotation velocity, linear acceleration, and magnetic field vectors. A pressure sensor

FIGURE 1

Gliding robotic fish “Grace” deployed in field tests. (a) Grace 1.0 after sampling oil concentration at the Kalamazoo River, Michigan; (b) Grace 1.0 sampling HABs at the Wintergreen Lake, Michigan; (c) Grace 2.0 tested at the Higgins Lake, Michigan, for potential application in acoustic telemetry of fish movement.



(a)



(b)



(c)

(Honeywell 40PC100G2A) is used to measure the depth, with one port connecting to the ambient water. A GPS (Garmin GPS 18x LVC) unit is used to provide the global position and the universal time, which is only effective when the gliding robotic fish surfaces. Grace is also equipped with a crude oil sensor (Turner Designs Cyclops-7 Crude Oil Sensor) and a temperature sensor. The sensor can be easily swapped to measure other environmental processes, such as chlorophyll, harmful algae, turbidity, rhodamine, etc. There is also a wireless communication unit (XBee Pro 900 XSC RPSMA) with the extruding antenna (900MHz Duck Antenna RP-SMA) at the top front, which is capable of communication for a distance up to 1.6 km in an ideal situation.

Three-Dimensional Steady Spiral and Its Differential Geometry Features

The three-dimensional motion control for gliding robotic fish, in terms of curve tracking, is very challenging because the influences of the control inputs on the robot's locomotion are strongly nonlinear and coupled. It is more convenient to look into the influence of control inputs on the robot's differential geometry features, such as curvature and torsion, because we can examine the relationship between those geometric characteristic parameters and the control inputs by studying the steady-state spiral motions of the robot.

We decompose an arbitrary three-dimensional curve into a set of continuously evolving spirals. In this way, at any point of the space curve,

there is an imaginary matching spiral curve with the same curvature and torsion. With this interpretation, instead of using the Euclidean positions, we will explore the task of three-dimensional curve tracking via designing and following continuously evolving spirals from the point of view of differential geometry.

Steady Spiral Motion

There are three control variables available to manipulate the robot's motion profile: the net buoyancy m_0 , the position of the movable mass r_p , and the tail angle δ .

From Zhang et al. (2013, 2016b), we know that, when all three controls are fixed at nonzero values, the gliding robotic fish will perform three-dimensional steady spiraling motion, where the yaw angle φ changes at a constant rate while the roll angle ϕ and pitch angle θ remain constant. In a steady spiral, the angular velocity has only one nonzero component, which is in the direction of gravity.

There are two important parameters in the spiraling motion: the turning radius R and the vertical speed V^v . By projecting the total velocity \boldsymbol{v} into the horizontal plane and the vertical direction, we can derive those two variables.

The steady-state spiraling is a relative equilibrium of the dynamic system. The steady-state spiral path can be completely described by six system states, including pitch angle θ , roll angle φ , angular velocity amplitude Ω , translational velocity amplitude V , angle of attack α , and sideslip angle β .

Differential Geometry Features of Spirals

In this section, we will look into the spiral curve from the point of view of elementary differential geometry. A

spiral/helix is a space curve with parametric equations

$$x_s | = r \cos t \quad (1)$$

$$y_s | = r \sin t \quad (2)$$

$$z_s | = ct \quad (3)$$

for $t \in [0, 2\pi]$, where r is the radius of the spiral and $2\pi c$ is the pitch of the spiral, a constant giving the vertical separation of the spiral's loops.

In the elementary differential geometry of a three-dimensional curve, curvature κ is the amount by which a geometric object deviates from being flat or the degree by which a geometric object bends, while torsion τ measures the departure of a curve from a plane or how sharply a curve twists. Any space curve can be completely described mathematically using curvature and torsion by Frenet-Serret formulas (Pressley, 2010; Shifrin, 2010).

The curvature of the spiral is given by

$$\kappa = \frac{r}{r^2 + c^2} \quad (4)$$

The torsion of a spiral is given by

$$\tau = \frac{c}{r^2 + c^2} \quad (5)$$

For a steady spiral, the curvature and torsion are constants with the above relationship with the radius and the pitch of the spiral, which are also constants.

Influence of Control Inputs on Spiral Trajectory

As for the spiral motion, the three control inputs, including the movable mass displacement r_p , the net

FIGURE 2

Trajectory characteristic parameters at different tail angles with $m_0 = 30$ g and $r_p = 0.5$ cm.

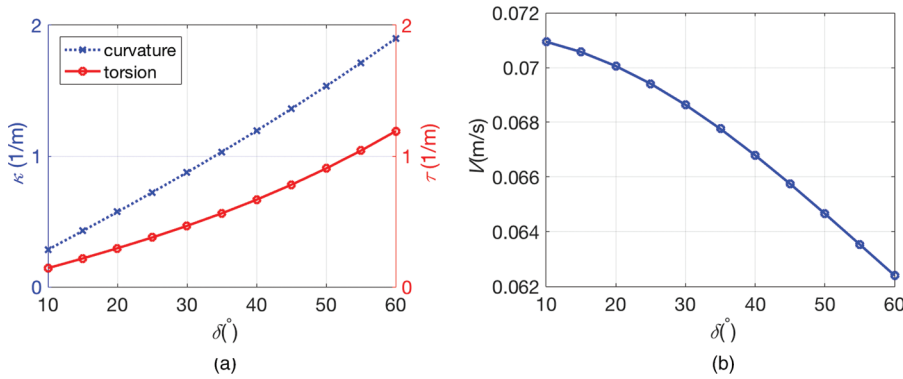
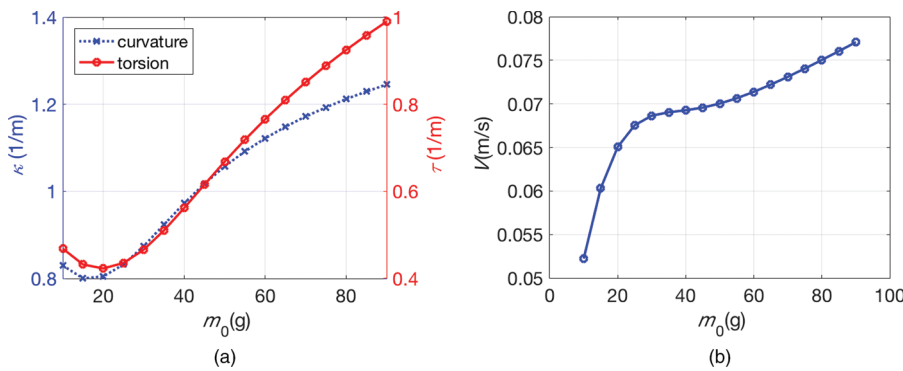


FIGURE 3

Trajectory characteristic parameters at different net buoyancy with $\delta = 30^\circ$ and $r_p = 0.5$ cm.

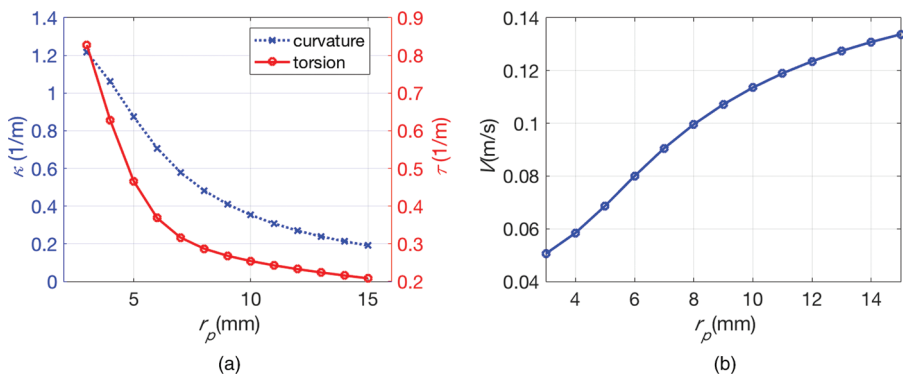


buoyancy m_0 , and the tail angle δ , have different influences on both the steady-state motion profile and the transient dynamics. In this paper, we focus on the influences of control

inputs on the steady-state spiral trajectory characteristics, which provide useful insight for path planning in three-dimensional curve tracking.

FIGURE 4

Trajectory characteristic parameters at different displacements of movable mass with $\delta = 30^\circ$ and $m_0 = 30$ g.



We study the relationship between three system control inputs and three trajectory characteristic parameters, including curvature κ , torsion τ , and total speed V , which are used to completely describe any three-dimensional trajectory. We conduct simulation with different sets of values of system control inputs and then record the corresponding steady-state spiral paths. The dynamic model used in the simulation was derived and detailed in (Zhang et al., 2016b).

Figure 2 shows the relationship between tail angle δ and the three trajectory characteristic parameters, while the net buoyancy m_0 and the displacement of movable mass r_p are fixed at 30 g and 0.5 cm, respectively. Simulation results of varying m_0 and r_p are shown in Figures 3 and 4. From those figures, we see that all control inputs have significant influence on the motion profile, although the degree of influence varies. For example, δ and r_p have greater influence on κ and τ than m_0 . Most relationships show monotonic trends, whereas nonmonotonic relationships appear between κ/τ and m_0 (Figure 3a). The simulation results of the influences of control inputs on the robot's spiral trajectory provide insight into the capability of three-dimensional maneuvering as well as the controller design for three-dimensional curve tracking.

Experiments

In experiments, Grace is remotely controlled via XbeePro communication to perform spiral motions with different control input values in the Neutral Buoyancy Research Facility at the University of Maryland (Figure 5). The whole spiral process is recorded using a Qualisys underwater motion capture system. The Qualisys

FIGURE 5

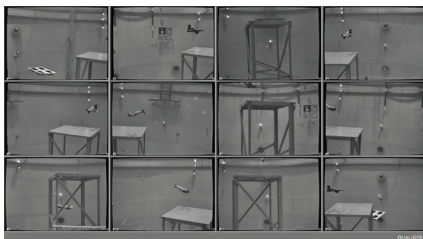
The gliding robotic fish “Grace” spiraling in Neutral Buoyancy Research Facility, University of Maryland.



system is suitable for a wide range of applications, such as ship design, naval research, fishing industry, and sports science. The motion capture system in our experiment features 12 underwater cameras around the water tank, with eight at a shallower depth and four at a deeper depth. Each camera captures the spiral motion from a different angle of view (Figure 6). The cameras are controlled through the Qualisys Track Manager software (QTM) and can be synchronized with external hardware. QTM takes full advantage of all the features of the camera, such as active filtering and the ability to stream 6 degree-of-freedom data in real-time. The system features high relative position accuracy of up to 2 mm. The robot is equipped with five markers, two on the wings

FIGURE 6

Snapshots of spiral motion with 12 underwater cameras from different angles of view using a Qualisys underwater motion capture system.



and three on the robot body, making an asymmetric geometry, which the motion capture system uses to identify the rigid body. Some of the robot’s states, such as linear and angular positions, can be measured and outputted using the motion capture system, and other states of the robot, including translational and angular velocities, can be estimated from those measurements.

Figures 7(a) and 7(b) show the results of comparison between the model prediction and the experimental results on the spiral curvature and torsion when δ is varied from 20° to 50° , with the values of m_0 and r_p fixed at 30 g and 0.5 cm, respectively. The results on the total speed of spiral are not presented as the influence of the tail angle on that variable is not very obvious as shown in Figure 2b. The spiral experiments at each set of control input values are conducted five times. The mean and standard deviation of κ and τ are provided with the error bar in the figures. Considering the current disturbance in the water tank due to the boundary effects and constantly active filtering system, the match between the model prediction and the experimental results is considered good.

The experiments for varying m_0 and r_p are not carried out and pre-

sented here because the speed and the gliding angle could be much increased and the robot would bump into the metal frame located in the center of the water tank (setup for other experiments and not removable).

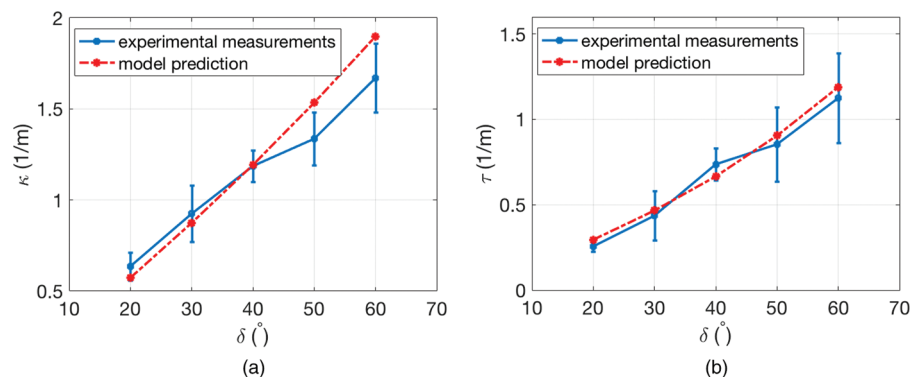
Three-Dimensional Curving Tracking Using Trajectory Characteristic Parameters

In this paper, we study one special case for three-dimensional locomotion to illustrate the idea of using spiral-based trajectory characteristic parameters (curvature κ , torsion τ , and speed V) for planning curve tracking. The three-dimensional trajectory is decomposed into trajectories of κ , τ , and V . Then by utilizing the knowledge about the relationship between those three parameters and the spiral control inputs (movable mass displacement r_p , net buoyancy m_0 , and tail angle δ), we adopt feedback and feedforward control algorithms to maneuverer the robot along the desired trajectory.

Due to the strong coupling of control inputs in the influence on the trajectory parameters, advanced nonlinear control algorithm is desirable

FIGURE 7

Model prediction and experimental results on spiral motion at different tail angles. The other two control inputs are fixed $m_0 = 30$ g, and $r_p = 0.5$ cm. (a) Curvature. (b) Torsion.



for satisfactory tracking performance. However, in this paper, we focus on a proof of concept for three-dimensional curve tracking using spiral-based parameters. Thus, based on the relationship between control inputs and spiral profiles shown in Figures 2–4, we design a combined feedforward and feedback controller as follows,

$$\delta | = K_p^\delta \Delta \kappa + K_I^\delta \int \Delta \kappa + \delta^{FF} \quad (6)$$

$$r_p | = K_p^{r_p} \Delta \tau + K_I^{r_p} \int \Delta \tau + r_p^{FF} \quad (7)$$

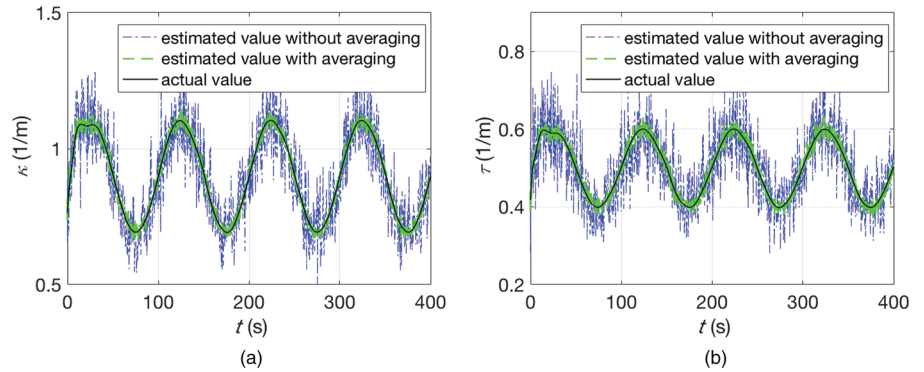
$$m_0 | = K_p^{m_0} \Delta V + m_0^{FF} \quad (8)$$

where Δ stands for the difference between the desired value and the actual value of the variable that follows. The PI controller coefficients are designed as $K_p^\delta = 0.5$, $K_I^\delta = 20$, $K_p^{r_p} = 0.5$, $K_I^{r_p} = 1$, and $K_p^{m_0} = 5$. We adopt PI control instead of PID control because the derivative term is typically sensitive to measurement noise, which is exactly the case for curvature and torsion feedback. The feedforward control δ^F , r_p^{FF} , and m_0^{FF} are obtained from the inverse mapping of the steady spiral profile using Newton's method (Zhang & Tan, 2014). The feedforward terms help to increase the convergence speed, whereas the feedback terms help to reduce the tracking error and enhance the system robustness.

The designed controller requires feedback information of curvature, torsion, and velocity. While robot velocity can be estimated by fusing sensor measurements from IMUs and depth pressure sensors, the curvature and torsion of the robot trajectory are difficult to obtain. Most of the existing research on curvature/

FIGURE 8

Simulation results of geometric parameter estimation. The averaging window size used is 25. (a) Curvature. (b) Torsion.



torsion estimation assumes knowing the robot's position (corrupted with some noise) and computes curvature and torsion using second-order and third-order derivatives of robot's position (Fumin Zhang et al., 2004). Even with very low position measurement noise, the differentiation opera-

tion on the noisy data often results in large estimation error.

In this paper, the steady-spiral geometry is utilized to compute the curvature and torsion of the robot trajectory. The radius r and pitch $2\pi c$ of the spiral curve are calculated as $r = V^b/\Omega$ and $c = V^v/\Omega$, respectively,

FIGURE 9

Simulation results for three-dimensional curve tracking. (a) Curvature. (b) Torsion. (c) Speed.

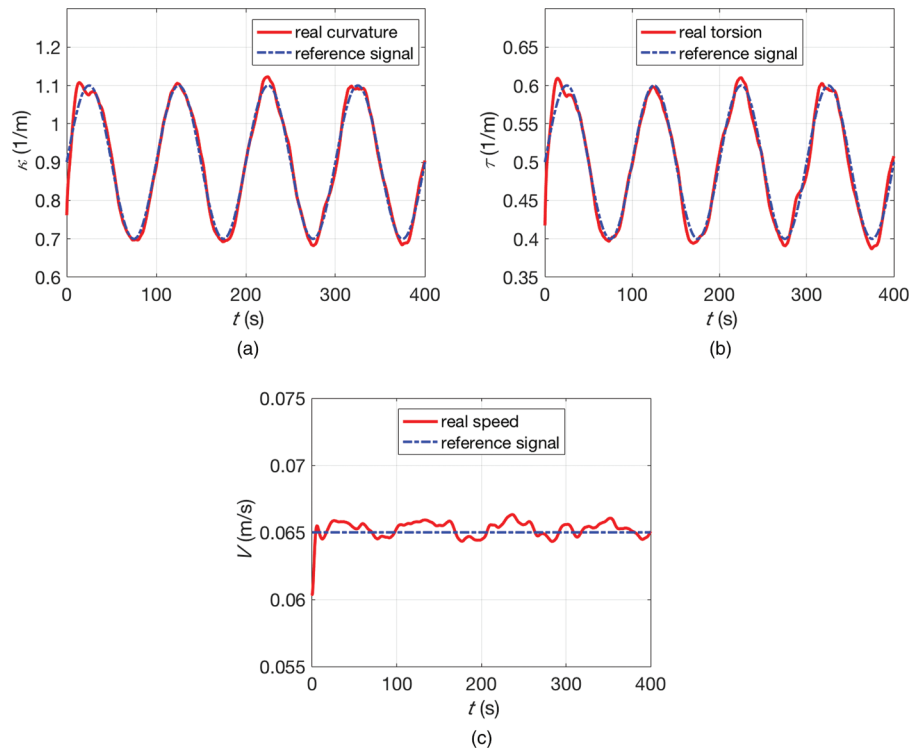
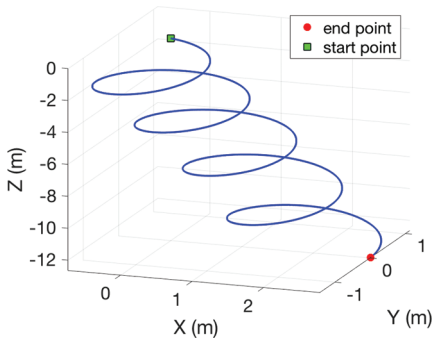


FIGURE 10

Actual trajectory of the robot in three-dimensional curve-tracking simulation.



where the horizontal speed V^h , the vertical speed V^v , and the angular speed Ω , estimated from IMU and pressure sensor measurements, are corrupted with Gaussian noises. The curvature κ and torsion τ are then

computed with the radius and pitch of spirals following Equations (4)–(5). To reduce the influences of noise, a moving average filter is applied to V^h , V^v , and Ω . Figure 8 shows the simulation results on curvature/torsion estimation with different averaging window sizes. As shown in the figure, the estimated values of κ and τ without averaging is too noisy to be used for curve tracking, whereas the estimated values of κ and τ with an averaging filter that has a window size of 25 is considered acceptable and used later in the curve-tracking simulation.

Figures 9–11 show the simulation results for a special case of three-dimensional curve tracking. The reference command of curvature and

torsion are sinusoidal functions, whereas the reference command of the total speed is a constant. The simulation results illustrate and validate the proposed idea of three-dimensional curve tracking using spiral-based trajectory characteristic parameters. On the other side, the simulation-tracking error also indicates the need of further nonlinear controller design for better tracking performance.

Conclusions

In this paper, we proposed a method for three-dimensional curve tracking for gliding robotic fish by following the trajectory characteristic parameters (curvature, torsion, and speed). First, we presented our lab-developed gliding robotic fish prototype. We also looked into three-dimensional steady-state spiral motion and its trajectory characteristics from the perspective of elementary differential geometry. The influences of control inputs on the spiral trajectory were studied through both simulation and experiments. A simulation example was demonstrated to illustrate the proposed concept.

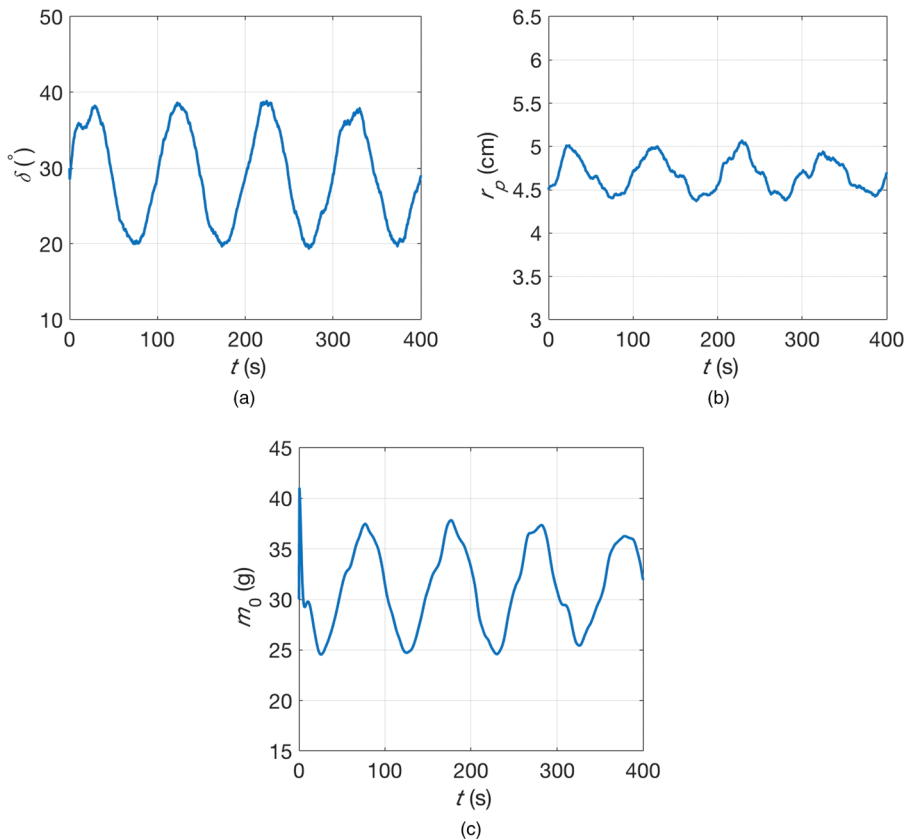
In future work, we will look into advanced nonlinear controller design for the three-dimensional curve-tracking problem and explore the effectiveness of the controller in experiments.

Acknowledgments

This work was supported in part by the National Science Foundation (IIS 0916720, IIS 1319602, IIP 1343413, CCF 1331852, ECCS 1446793). The authors would like to thank Dr. Derek A. Paley and Nitin Sydney from the University of Maryland for their help in conducting experiments in the Neutral Buoyancy Research Facility.

FIGURE 11

Simulation trajectories of the three control inputs. (a) Tail angle. (b) Movable mass displacement. (c) Net buoyancy.



Corresponding Author:

Feitian Zhang

Department of Electrical and
Computer Engineering, George Mason
University, 4400 University Drive,
MSN 1G5, Fairfax, VA 22033
Email: fzhang9@gmu.edu

References

- Bhatta**, P., & Leonard, N.E. 2008. Nonlinear gliding stability and control for vehicles with hydrodynamic forcing. *Automatica*. 44(5):1240-50. <https://doi.org/10.1016/j.automatica.2007.10.006>.
- Chen**, Z., Shataru, S., & Tan, X. 2010. Modeling of biomimetic robotic fish propelled by an ionic polymer metal composite caudal fin. *IEEE-ASME T Mech*. 15(3):448-59. <https://doi.org/10.1109/TMECH.2009.2027812>.
- Graver**, J.G. 2005. *Underwater Gliders: Dynamics, Control, and Design*. Princeton, NJ: Princeton University.
- Leonard**, N.E., & Graver, J.G. 2001. Model-based feedback control of autonomous underwater gliders. *IEEE J Oceanic Eng*. 26(4):633-45. <https://doi.org/10.1109/48.972106>.
- Mahmoudian**, N., Geisbert, J., & Woolsey, C. 2010. Approximate analytical turning conditions for underwater gliders: Implications for motion control and path planning. *IEEE J Oceanic Eng*. 35(1):131-43. <https://doi.org/10.1109/JOE.2009.2039655>.
- Mitchell**, B., Wilkening, E., & Mahmoudian, N. 2013. Developing an underwater glider for educational purposes. In *Proceedings-IEEE International Conference on Robotics and Automation* (pp. 3423-8). <https://doi.org/10.1109/ICRA.2013.6631055>.
- Morgansen**, K.A., Triplett, B.I., & Klein, D.J. 2007. Geometric methods for modeling and control of free-swimming fin-actuated underwater vehicles. *IEEE T Robot*. 23(6):1184-99. <https://doi.org/10.1109/LED.2007.911625>.
- Phamduy**, P., Legrand, R., & Porfiri, M. 2015. Robotic Fish: Design and characterization of an interactive iDevice-controlled robotic fish for informal science education. *IEEE Robot Autom Mag*. 22(1):86-96. <https://doi.org/10.1109/MRA.2014.2381367>.
- Pressley**, A.N. 2010. *Elementary differential geometry*. London, UK: Springer.
- Sherman**, J., Davis, R.E., Owens, W.B., & Valdes, J. 2001. The autonomous underwater glider "Spray". *IEEE J Oceanic Eng*. 26(4):437-46. <https://doi.org/10.1109/48.972076>.
- Shifrin**, T. 2010. *Differential geometry: A first course in curves and surfaces*. University of Georgia. 1:125.
- Tan**, X. 2011. Autonomous robotic fish as mobile sensor platforms: Challenges and potential solutions. *Mar Technol Soc J*. 45(4):31-40. <https://doi.org/10.4031/MTSJ.45.4.2>.
- Webb**, D.C., Simonetti, P.J., & Jones, C.P. 2001. SLOCUM: An underwater glider propelled by environmental energy. *IEEE J Oceanic Eng*. 26(4):447-52. <https://doi.org/10.1109/48.972077>.
- Zhang**, F., Ennasr, O., Litchman, E., & Tan, X. 2016a. Autonomous sampling of water columns using gliding robotic fish: Algorithms and harmful-algae-sampling experiments. *IEEE Syst J*. 10(3):1271-81. <https://doi.org/10.1109/JSYST.2015.2458173>.
- Zhang**, F., Lagor, F.D., Yeo, D., Washington, P., & Paley, D.A. 2015. Distributed flow sensing for closed-loop speed control of a flexible fish robot. *Bioinspir Biomim*. 10(6):65001. <https://doi.org/10.1088/1748-3190/10/6/065001>.
- Zhang**, F., O'Connor, A., Luebke, D., & Krishnaprasad, P.S. 2004. Experimental study of curvature-based control laws for obstacle avoidance. *IEEE Int Conf Robot*, 2004. 3849-54. <https://doi.org/10.1109/ROBOT.2004.1308868>.
- Zhang**, F., & Tan, X. 2014. Three-dimensional spiral tracking control for gliding robotic fish. In *Proceedings of the IEEE Conference on Decision and Control* (Vol. 2015-Feb, pp. 5340-5). Los Angeles, CA: IEEE. <https://doi.org/10.1109/CDC.2014.7040224>.
- Zhang**, F., & Tan, X. 2015. Passivity-based Stabilization of Underwater Gliders with a Control Surface. *J Dyn Syst-T ASME*. 137(June):1-13. <https://doi.org/10.1115/1.4029078>.
- Zhang**, F., Thon, J., Thon, C., & Tan, X. 2014. Miniature underwater glider: Design and experimental results. *IEEE-ASME T Mech*. 19(1):394-9. <https://doi.org/10.1109/TMECH.2013.2279033>.
- Zhang**, F., Zhang, F., & Tan, X. 2016b. Tail-enabled spiraling maneuver for gliding robotic fish. *J Dyn Syst-T ASME*. 136(4):1-8. <https://doi.org/10.1115/1.4026965>.
- Zhang**, S., Yu, J., Zhang, A., & Zhang, F. 2013. Spiraling motion of underwater gliders: Modeling, analysis, and experimental results. *Ocean Eng*. 60:1-13. <https://doi.org/10.1016/j.oceaneng.2012.12.023>.